LARGE SCALE FIELD TESTING OF HILLSLOPE DEBRIS FLOWS RESULTING IN THE DESIGN OF FLEXIBLE PROTECTION BARRIERS

Louis Bugnion[1], Albrecht von Boetticher[2] and Corinna Wendeler[3]

ABSTRACT

In a disused quarry in Veltheim, Switzerland, we release up to 50 m^3 debris material down a 41 m long and 30° steep channel. The muddy and erosive flows obtained are similar to hillslope debris flows observed in nature. 30 m downstream from the retaining basin, we measure the front velocity, the flow height and the impact pressure on obstacles (see Fig. 1). At the lower end of the channel a flexible test barrier is installed. Load cells built in the support ropes of the barrier measure the forces during impact. The objective is to relate the flow parameters to the loads measured in the different elements of the barrier. The software FARO (Volkwein 2004) modelling the flexible barrier is used to compute barrier deformations from the impact pressures. The load model relating the flow parameters to the impact pressures is the object of the present paper. Data and computations for over 20 tests allow us to validate the flexible barrier design method.

Keywords: hillslope debris flow, large scale test, impact pressure coefficient, flexible protection barrier, one surge model, OPEN FOAM

METHODS

To design protection measures against landslides or debris flows, few approaches exist in Switzerland. Flexible barriers against debris flows are designed using a so called multi-surge model. Each surge consists of a hydrostatic and a dynamic pressure component. The dynamic load is expressed as the product of the impact velocity square with the flow density and with an impact coefficient c that depends on the material properties (Wendeler 2008). The coefficient c ranges between c = 0.7 for watery flows and c=1.0 for viscous flows monitored at the Illgraben torrent in Switzerland. In the Swiss guideline the impact coefficient for mudflows is set to c = 2.0 for stiff structures (Egli 2005). The question to be asked is if the difference between the impact coefficient values relies on the nature of the obstacle, flexible structure on the one hand and stiff structure on the other hand or on the flow/obstacle geometry. In our tests, the material density ranges between 1760 and 2110 kg/m^3 and the front velocity varies between 2 and 13 m/s. The flow heights are of the same order of magnitude as the size of the obstacles. The impact coefficients obtained range between 0.3 and 1.2 with median values of 0.65 and 0.78 for the large and small obstacles respectively. These values are used in the procedure for the barrier design which will be described in the following. Two different approaches are explained and compared; the first one is the simple one surge model derivated from the multi surge model for debris flow barriers (Wendeler 2008), the second one uses the software OpenFOAM to compute the interaction between the undisturbed flow and the flexible barrier.

[1] PhD Louis Bugnion. WSL, Switzerland
[2] PhD Albrecht von Boetticher. WSL, Switzerland
[3] Dr. Corinna Wendeler. Geobrugg AG, Aachstrasse 11, 8590 Romanshorn, Switzerland (e-mail: corinna.wendeler@geobrugg.com)

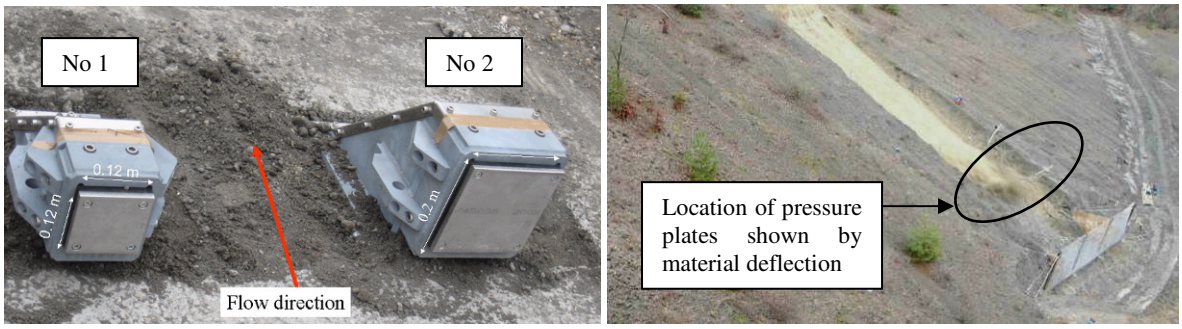

Fig. 1 Pressure plates measuring impact pressure (left side) and debris flow front impacting the pressure plates (right side).

IMPACT PRESSURE MEASUREMENTS

As mentioned above, we release 50 m^3 of debris saturated with water on a 41 m long, 8 m wide and 30° inclined channel. The channel is excavated to the bedrock and the 1 to 2 m high sediment sidewalls make an angle of about 120° with the channel bed. The material mixture is prepared at a nearby location and transported by truck to the retaining basin located at the top end of the channel. At the lower end of the channel, a 15 m long and 3.5 m high flexible barrier stops the flow. 30 m downstream of the retaining basin in the centre of the channel, 2 pressure plates are installed perpendicular to the flow direction. They have a square surface with 12 cm and 20 cm side length respectively. The force sensor is protected from the flowing material by two steel plates separated by an elastomer layer and measures with a 2 kHz frequency. In addition to the pressure plates, distance sensors located above the channel record the depth and are used to compute the front velocity of the undisturbed flow. We take material samples in the reservoir and in the deposit which are analysed in laboratory to determine grain-size distribution, density and water content.

Here we present the impact pressure signal measured on the small pressure plate during release 7.1 (first release of test 7). The maximum impact pressure value is used in the one surge load model as well as for comparison in the OpenFOAM load model. The mass fraction (of the solid phase) of fines (grain size $d < 0.063$ mm) was 34%, the mass fractions of sand ($d < 2$ mm) and gravel ($d < 60$ mm) were both 33%. The water content attained 20% (mass fraction) and the density was equal 1760 kg/m^3. The flow front velocity 26 m downstream of the reservoir was equal to 8.6 m/s and the maximum flow depth at that location was 0.3 m. In Fig. 1, the raw pressure signal (a), the mean pressure signal averaged over 0.05 s time intervals and the standard deviation of the pressure signal over 0.05 s time intervals (b) are represented.

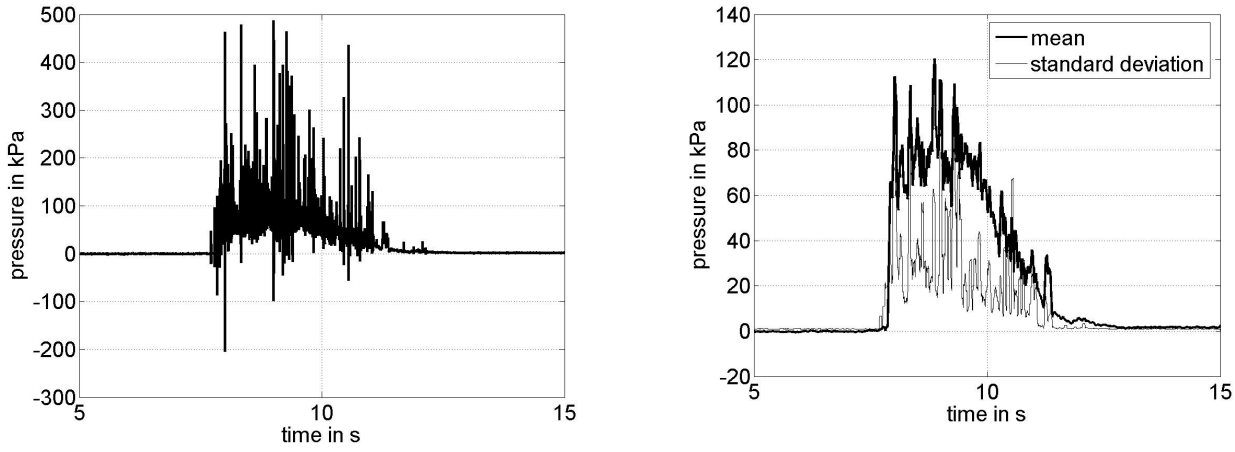

(a) (b)

Fig. 2 Raw (a), mean and standard deviation (b) of pressure signal during first release of release 7.1

The highest values of the mean pressure signal (see Fig. 2 (b)) are measured during the first 2 s of the impact and range between 100 and 120 kPa (the maximum impact pressure in the flow front is 112.5 kPa). From the front velocity and density we can compute the impact coefficient c = 0.86. In the flow tail the mean pressure decreases regularly to a static pressure value close to zero. The fast oscillations of the pressure signal in the raw pressure signal (Fig. 2 (a)) are related to vibrations of the pressure plate under the effect of hard contacts with solid grains composing the flow mixture. The averaging time interval of 0.05 s was chosen on the base of calibration tests and corresponds to the maximum duration of the pressure plate vibration after a hard contact with a steel ball. The standard deviation of the pressure signal is proportional to the mean of the pressure signal and the proportionality coefficient depends on the pressure plate dimensions (for the small pressure plate ~ 0.4).

ONE SURGE LOAD MODEL FOR SL BARRIER DESIGN

We model the flexible barrier with the finite element software FARO developed at the ETH Zürich (Volkwein 2004). The code was modified and enlarged for pressure loads caused by debris flows, snow gliding and shallow landslides in Wendeler 2008. In a first step we calculate the barrier loads during the impact consecutive of release 8.1. The forces measured in the barrier elements are plotted in Fig. 3. From camera recordings, we observed the maximum deformation of the flexible barrier 2 s after the impact of the flow front coinciding with the peak loads in the support ropes. The filling process lasts for about 5 s. The input parameters for the calculation are the flow height, the impact width and the maximum impact pressure measured on the obstacles. In the model, the impact pressure is increased linearly from 0 to the maximum impact pressure value of 72.9 kPa between t = 0 s and t = 2 s. Between t = 2 s and t = 5 s the impact pressure is decreased linearly to the static pressure value. The material is not drained so that the static pressure acts over the total filling height of 1.8 m. The computation results for the forces in the support ropes agree with the force cells measurements within a range of 15% (see Fig. 3).

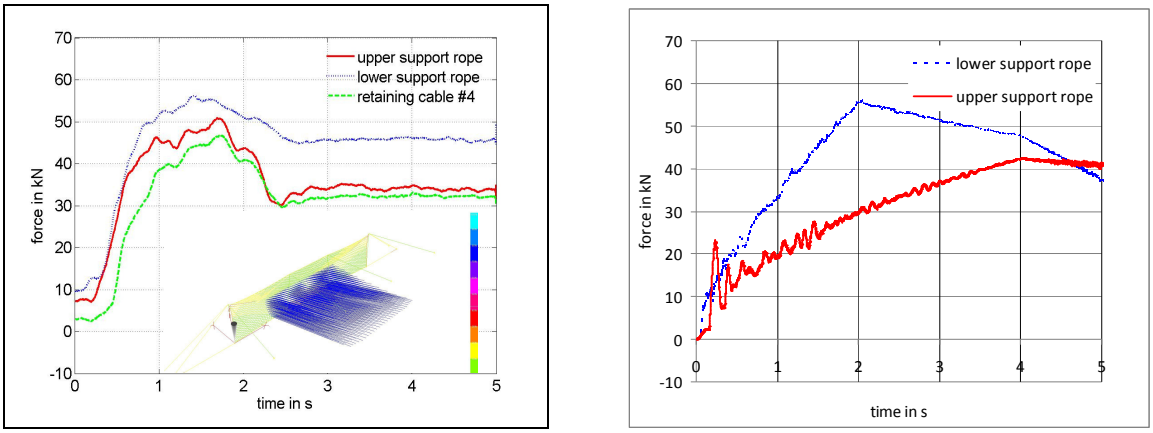

Fig. 3 Loads measured in the support ropes (left side) and forces computed with FARO software (right side) for release 8.1.

The releases of test 7 were easier to model with OpenFOAM because there were no guiding walls installed yet (see explanation in chapter impact simulation with OpenFOAM). Thus releases 7.1 and 7.2 are also modelled with the simplified one surge load model in order to be able to compare the results with the OpenFOAM load model. The maximum pressure was equal to 112.5 kPa and the maximum flow height at the location of the pressure plate was 0.3 m. The complete filling process took around 4 s. In the calculation the pressure at the end of the filling process is set to the static value computed from the barrier filling height and material density. For release 7.2 the maximum impact pressure measured by the small pressure plate was 75.2 kPa and the maximum flow height was 0.3 m.

RESULTS ONE SURGE LOAD MODEL

Table 1 and 2 show the comparison between measured load forces and forces obtained using the single surge load model. The measurement error of the load forces ranges between 0.5% and 3% at 100 kN depending on the force cell.

Tab. 1 Measured peak loads in the upper and lower support ropes for release 7.1 and 7.2 in comparison with results of the one surge load model

Release	Lower rope, measured [kN]	Lower rope, modelled [kN]	Upper rope, measured [kN]	Upper rope, modelled [kN]
7.1	85	95	82	60
7.2	120	130	115	120

Tab. 2 Measured peak loads in the retaining cables of the impact and border fields for release 7.1 and 7.2 in comparison with results of the one surge load model

Release	Retaining cable impact field, measured [kN]	Retaining cable impact field, modelled [kN]	Retaining cable border field, measured [kN]	Retaining cable border field, modelled [kN]
7.1	60	30	40	20
7.2	120	120	120	100

For release 7.1, the one surge load model together with the software FARO overestimates the peak load in the lower support rope by 11%. The peak load in the upper support rope is underestimated by 25%. The peak loads in the retaining ropes are all underestimated by the model. The overestimation of the bottom support rope peak load can be explained by the presence of the erosion control apron. The erosion control apron is a mesh fixed to the lower support rope and anchored to the ground with earth nails. It is not considered in the barrier modeling and contributes to the reduction of the loads in the lower support rope. The peak load in the upper support rope is underestimated by 25%. One possible reason is that the weight of the sag made by the filled barrier to the front is not modeled. Only the impact pressure in the flow direction and the static pressure due to the height of the retained material are taken into account in the model. In the reality, the barrier forms a belly to the front whose weight is supported by the posts and by the upper support rope. The strong underestimation of the retaining cable at the impact field at Test 7.1 is not due to the model but to the fact, that one mesh got caught at the top edge of the post leading to a high local force introduction to the post and its retaining cable. In the second release the dynamic impact pressure transmitted to the barrier fits more or less good to measured rope force. Also the maximum load values of the retaining ropes can be modeled with this simplified model. The influence of the erosion control apron at the bottom support ropes plays no role any more in the physical process of second hit. Also the top support ropes are getting more influenced by the dynamic impact force, because the flow is overflowing the already deposited material behind the barrier and is hitting the barrier in a height of 1.3 m over the bottom. The static load of the material weight in the belly is playing a role besides compared with the dynamic hit of second surge with a max. peak load of 100 kN/m^2.

COUPLED IMPACT SIMULATION WITH THE OPEN SOURCE SOFTWARE OPENFOAM

The impact area at the barrier was modelled by using the open source CFD code OpenFOAM. A two-phase solver 'interFoam' was used to simulate the impact material and the air, representing the free surface by the 'Volume of Fluid' method. In a second step, the explicit weak coupling of the impact fluid dynamics to a structure code representing the flexible barrier was carried out. This setup is based on the 'interDyMFoam' solver, which can handle dynamic mesh movements additionally to the 'interFoam' solver. The barrier is simulated using the discrete finite element code FARO developed for modelling rockfall protection barriers. It receives from OpenFOAM the local forces due to the local

impact pressures at each node of the barrier mesh and sends back the corresponding local deformations of the barrier that act as a boundary deformation at the OpenFOAM domain.

The OpenFOAM domain is characterized by an inlet according to the front flow height that introduces the flow material as a block with time dependent inflow velocity. Half of the material is introduced with the given front flow velocity along one third of the total inflow time, then the inflow velocity is decreased to zero over the following two thirds of the total inflow time. With this simple inflow condition, the development of the impact over time is in accordance with the measured time series for different experiments at the Veltheim test site.

The introduced material with constant flow velocities over height would conflict with a no-slip boundary condition at the slope. For that reason, the first part of the slope near the inlet is modelled with a full slip boundary condition, followed by a no slip boundary condition for the rest of the slope which allows developing a velocity profile. A minimal viscosity is introduced, that assures that the material does not accelerate until it reaches the barrier. This way, the mean front velocity given as input becomes the front velocity $v_{contact}$ that hits the barrier. Fig. 4 shows a longitudinal section of the modelled impact room with the barrier at the left and inlet at the right, where the input parameters of front velocity and density v_{in}, $\rho_{in,}$ and flow height h_{in} are illustrated.

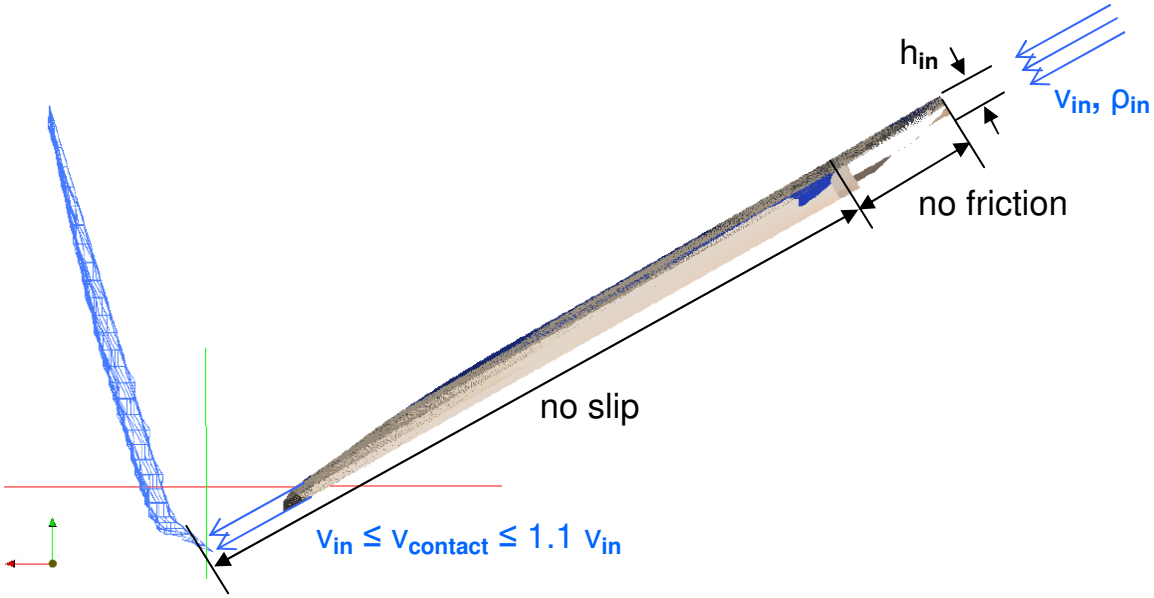

Fig. 4 Longitudinal section of the simulated impact room

Rheology law for the modelled impact material

For the representation of the impact material with a single phase, a Herschel-Bulkley rheology law was chosen, with a successful automated linking of the Herschel-Bulkley parameters to the shares of silt, clay, sand and gravel and to the water content and average density of the solid. This way, the shear thinning behavior of the impact material is taken into account with its decisive influence on the filling process. While giving good results when simulating the barrier forces for the different tests carried out at Veltheim, the strong shear gradient of the simulated flow at the sides of the pressure plate combined with neglecting the impact of grains with sizes up to 10 cm cause an underestimation of the local viscosity and miss the local density peaks of the impact material. As a consequence, the simulated rigid impact pressures of the small pressure plate are underestimated (Fig. 5).

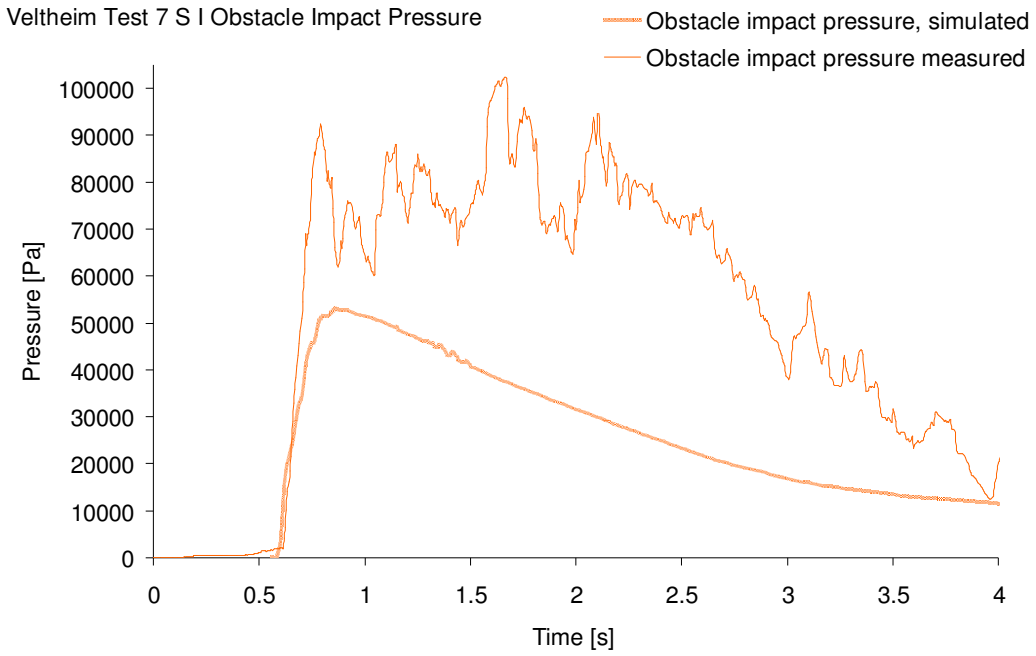

Fig. 5 Time series of measured and simulated pressures at the small pressure plate

Comparison of simulated and measured rope forces for the Fluid-Structure Interaction model

The Barrier is fixed by an upper and lower support rope holding the net and retaining ropes that keep the posts in position. Fig. 6 shows the comparison of the measured and simulated rope forces of the first shot of test number 7. Peak forces and the time distribution of forces of the support ropes are in good accordance with the measured values, while retaining forces are underestimated. The retaining rope of the impact field of test 7.1 is not representative because one mesh got caught at the top of the post leading to high local forces at the retaining cable. In later tests, sidewalls made out of plywood avoided the flow around the barrier. As a consequence, the inner retaining rope at first impact tests of such simulations fitted the measured values with 30% accuracy.

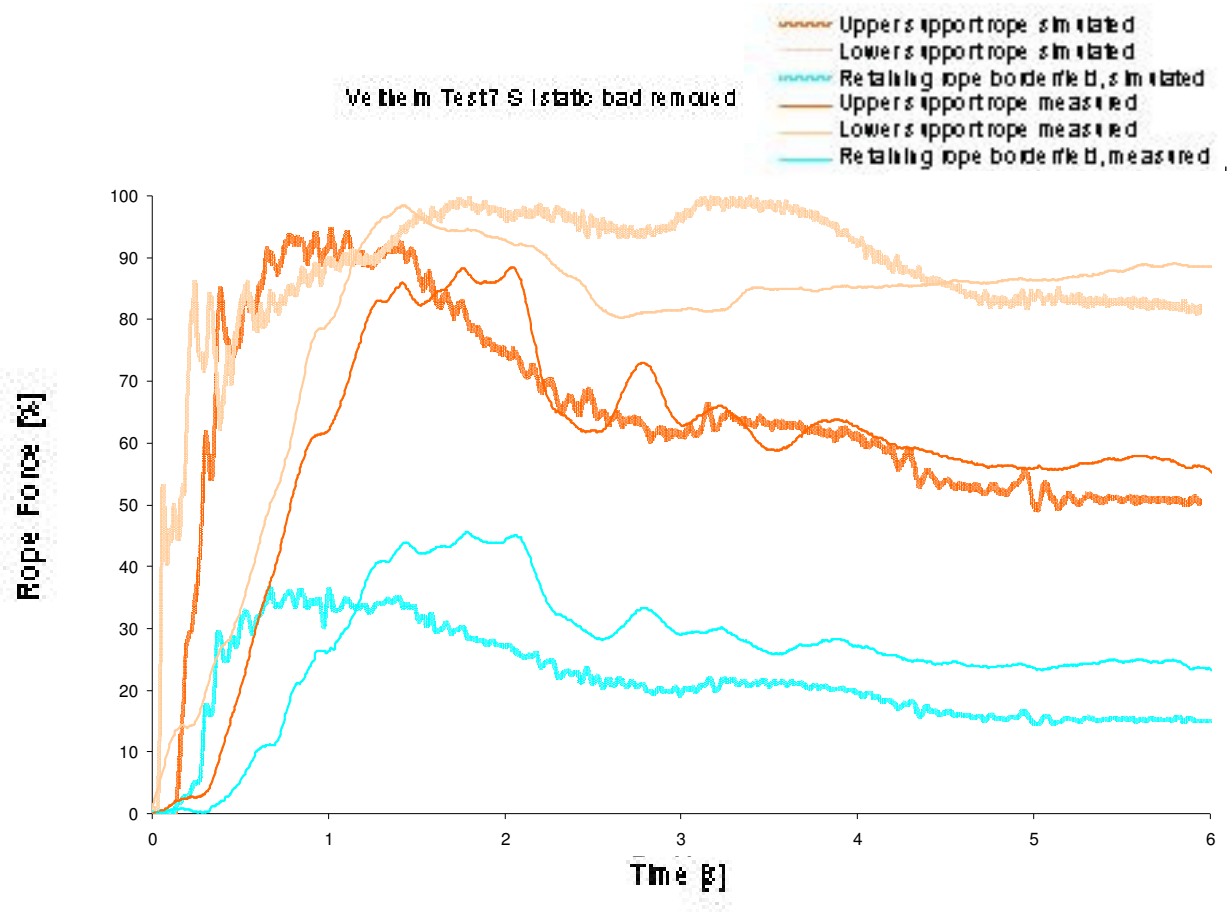

Fig. 6 Time series of measured and simulated rope forces at the barrier

Table 3 and 4 show the comparison between measured load forces and forces obtained using the coupled model. The measurement error of the load forces ranges between 0.5% and 3% at 100 kN depending on the force cell.

Tab. 3 Measured peak loads in the upper and lower support ropes for release 7.1 and 7.2 in comparison with results of the coupled model, static load included

Release	**Lower rope, measured [kN]**	**Lower rope, modelled [kN]**	**Upper rope, measured [kN]**	**Upper rope, modelled [kN]**
7.1	85	86	82	87
7.2	120	130	115	120

Tab. 4 Measured peak loads in the retaining cables of the impact and border fields for release 7.1 and 7.2 in comparison with results of the coupled model, static load included

Release	**Retaining cable impact field, measured [kN]**	**Retaining cable impact field, modelled [kN]**	**Retaining cable border field, measured [kN]**	**Retaining cable border field, modelled [kN]**
7.1	60	21	40	33
7.2	120	84	120	74

DISCUSSION

The large scale field testing of hillsolpe debris flows made it possible to develop and validate impact models for the loading of flexible protection barriers. The single surge load model is a valid simple approach to gain an estimation of the peak forces together with a representation of the barrier using FARO. For a detailed reproduction of the filling process and the interaction between barrier and impact flow, the coupled model with OpenFOAM and FARO is a convincing tool that allows studying the dynamic behavior of all structure parts in detail, delivering insight into the processes involved. It can increase the understanding of the coupled system behavior and point out critical parts. The optimization of the structure design as well as the detailed study of protection barriers adapted to complex hillslope geometries is supported by the coupled model.

REFERENCES

Bugnion L., McArdell B., Bartelt P., Wendeler C., (2011). Measurements of Hillslope Debris Flow Impact Pressure on Obstacles, Landslides, in press.

Egli T. (2005). Wegleitung der kantonalen Gebäudeversicherungen - Objektschutz gegen gravitative Naturgefahren.

Volkwein A. (2004). Numerische Simulation von flexiblen Steinschlagschutzsystemen, Dissertation, ETH-Zürich.

Wendeler C. (2008). Murgangrückhalt in Wildbächen – Grundlagen zu Planung und Berechnung von flexiblen Barrieren. Dissertation, ETH-Zürich.